

Localized Therapeutic Release via an Amine-Functionalized Poly-*p*-xylene Microfilm Device

Erik M. Robinson,[†] Robert Lam,[‡] Erik D. Pierstorff,^{†,‡} and Dean Ho^{*,†,‡,§}

Department of Biomedical Engineering, Northwestern University, Evanston, Illinois 60208, Department of Mechanical Engineering, Northwestern University, Evanston, Illinois 60208, and Robert H. Lurie Comprehensive Cancer Center, Northwestern University, Chicago, Illinois 60611

Received: June 15, 2008; Revised Manuscript Received: July 30, 2008

Developing biocompatible polymeric platforms for drug delivery with enhanced localized activity represents a key facet of advanced interventional therapy. In this work, the drug-eluting potential of an amine-functionalized poly-*p*-xylene commonly known as Parylene A (4-amino(2,2)paracyclophane) was conducted with the microfilm device consisting of a primary base layer, drug film, and a secondary eluting layer presenting exposed amine groups which enhance the range of modifications that can be incorporated into the film. The murine macrophage cell line RAW 264.7 served as a cellular response to dexamethasone, a synthetic anti-inflammatory glucocorticoid and doxorubicin, an anticancer therapeutic. Decreased expression of NF κ -B-mediated cytokines Interleukin-6 (IL-6) and Tumor Necrosis Factor- α (TNF α), resultant DNA fragmentation, and spectroscopic analysis revealed the efficient and localized drug-eluting properties of the Parylene A polymeric bilayer.

Introduction

A broad range of biomaterials has been explored for translational applications in tissue engineering and drug delivery. Of these materials, the family of poly-*p*-xylenes, commonly known as parylene, is a widely accepted coating for medically implanted devices due to its biocompatibility^{1–3} (USP approved Class VI polymer). The nature of the chemical deposition process (CVD), through which the polymerization of parylene takes place, allows for the formation of a conformal barrier⁴ between the medical device and exterior environment. Another advantage to the deposition process is that it occurs at room temperature,⁵ preserving device function. Present day applications of parylene derivatives such as Parylene C (dichloro(2,2)paracyclophane) and Parylene N ((2,2)paracyclophane) include a range of devices from catheters⁶ to stents.⁷ Recent efforts to supplement the integration of parylene-coated medical devices by applying alternative drug-conjugated degradative polymeric coatings to the parylene surface have been successful in the fabrication of drug-eluting stents.^{7,8} These multipolymeric coatings complement the biomaterial platform to a significant extent. Improving upon existing functionalization methods either through a physical, biological, or material approach will further aid device integration.⁹ Here, we demonstrate the novel application of the amine-activated Parylene A platform as the backbone for microfilm device fabrication. As a biostable and localized drug delivery platform, the bilayer device serves as a catalyst for potential applications in sustained

drug release for enhanced efficacy in drug release continuity and treatment potency.

Experimental Methods

Substrate Preparation. Plain glass slides were sterilized in 70% ethanol and pretreated with A-174 Silane (SCS Coatings, Indianapolis, IN) adhesion promoter according to manufacturer's protocol. Approximately 2.0 g of Parylene A (Uniglobe Kisco, White Plains, NY) was loaded into a parylene deposition system (PDS) 2010 LABCOTER 2 (SCS Coatings). The deposition took place under previously indicated conditions.^{10,11} Application of the drug to the base layer of Parylene A was accomplished via desiccation of 150.0 μ g of dexamethasone (Sigma Aldrich, St. Louis, MO) or 37.5 μ g of doxorubicin (U.S. Pharmacopeia, Rockville, MD) under a laminar flow hood. A second layer of 150 mg of Parylene A was deposited over the drug films to produce the eluting layer.

Cell Culture Conditions. RAW 264.7 murine macrophage (ATCC Manassas, VA) cells were grown in DMEM media (Mediatech Inc., Herndon, VA) supplemented with 10% FBS (ATCC) and 1% penicillin/streptomycin (Lonza, Walkersville, MD). Investigation of inflammation pathways utilized the lipopolysaccharide, 5 ng/mL, (Sigma Aldrich) and resultant expression of IL-6 and TNF α genes. Analysis of cellular apoptosis was accomplished using agarose electrophoresis of DNA fragmentation.

Quantitative RT-PCR. RNA isolation was accomplished utilizing TRIzol reagent (Invitrogen Corporation, Carlsbad, CA) per the manufacturer's guidelines. cDNA was synthesized using the iScript Select cDNA Synthesis Kit (Bio-Rad, Hercules, CA). PCR was done using SYBER Green detection reagents (Quanta Biosciences, Gaithersburg, MD) and appropriate primers for IL-6, TNF- α , and β -Actin (Integrated DNA Technologies, Cor-

* To whom correspondence should be addressed. Address: 2145 Sheridan Rd, Evanston, IL 60208. Phone: (847) 467-0548. Fax: (847)491-3915. E-mail: d-ho@northwestern.edu.

[†] Department of Biomedical Engineering.

[‡] Department of Mechanical Engineering.

[§] Robert H. Lurie Comprehensive Cancer Center.

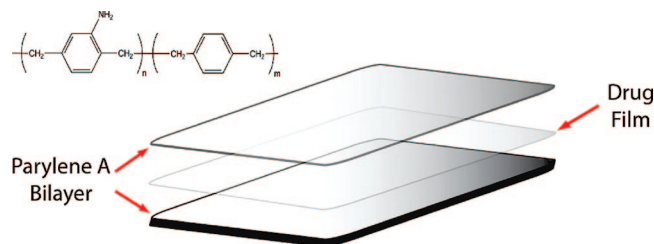


Figure 1. Structure of Parylene A (diX-A) and proposed model of the nanoscale drug-eluting Parylene A microfilm device. The base layer of parylene supports the drug film, while the secondary layer acts as the elution element, allowing release of the drug into a localized environment. Application of additional layers and/or differing therapeutic agents will result in a multifunctional nanoscale drug-eluting film.

alville, IA). Samples were amplified using a MyiQ real-time PCR detection system (Bio-Rad).

Electrophoretic Assay. Cells were washed with PBS wash and removed from the substrate. Cells were lysed using a cell lysis solution (10 mM tris-HCL, pH 8.0, 10 mM EDTA, 1% Triton X-100) and incubated with RNase and proteinase K. DNA was extracted using a 2% isoamyl alcohol (25:24:1) solution and precipitated in isopropanol. The remaining pellet was washed in 70% ethanol and resuspended in DEPC water. DNA fragmentation was characterized via a 0.8% agarose gel using sodium borate buffer¹² and ethidium bromide staining.

Spectroscopic Analysis. Microscope glass slides were cut to size and coated with a primary base layer of Parylene A as described previously; 0.25 mg of doxorubicin (U.S. Pharmacopeia) was desiccated onto the individual glass sections, and a secondary eluting layer of Parylene A (150 mg) was deposited. Samples were placed in a 12 well plate immersed in 1.0 mL of PBS for 10, 20, and 40 min and 1, 4, and 24 h increments. After each time point, the solution was removed, and the drug eluting glass disks were transferred to a vacant well and replenished with 1.0 mL of PBS. Remaining solutions were analyzed in a DU Series 700 UV/vis scanning spectrophotometer (Beckman Coulter, Fullerton, CA).

Surface Characterization. Parylene A substrates were imaged utilizing an Asylum MFP3D atomic force microscope (AFM) (Santa Barbara, CA). Each sample consisted of a 2 g Parylene A base layer, with an additional 150 mg applied to one substrate as described previously. Image dimensions were $20 \mu\text{m} \times 20 \mu\text{m}$. Contact mode imaging at line scan rates of $22 \mu\text{m/s}$ were performed at room temperature with an Olympus TR800PSA $200 \mu\text{m}$ length silicon nitride cantilever (Melville, NY).

Results and Discussion

In an effort to expand upon the capability of differentially functionalized poly-*p*-xylene derivatives, an examination as to the drug-eluting potential of parylene was conducted. This investigation centered on an amine-functionalized parylene (4-amino(2,2)paracyclophane) commonly known as Parylene A (commercially as diX-A). The deposition of Parylene A occurred in a two-step fashion wherein a coating of dexamethasone [DEX] (anti-inflammatory agent) or doxorubicin [DOX] (anti-cancer therapeutic) was dispersed between a primary base layer and a secondary elution layer. Illustrated in Figure 1 is a schematic representation of the proposed device. The polymerization reaction of the secondary layer allows for the release of the therapeutic agents examined. The release of the underlying drug is accomplished by restricting the amount of polymer

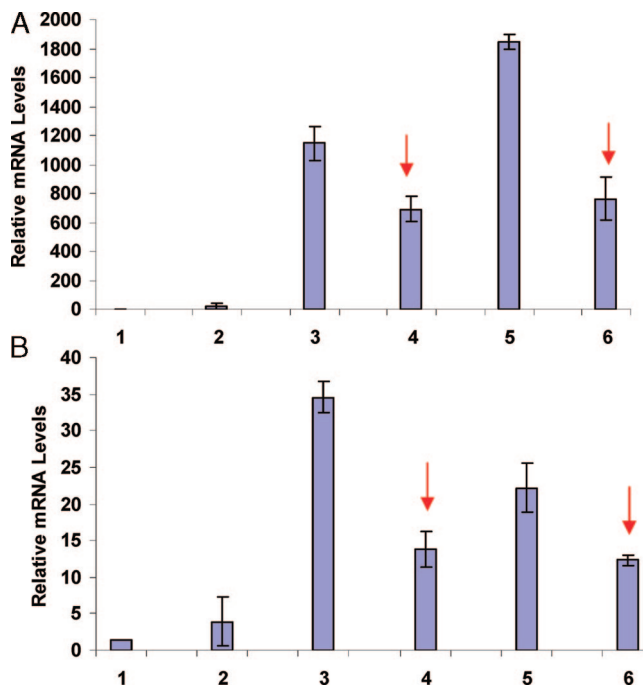


Figure 2. (A) Gene expression of inflammatory cytokine Interleukin-6 (IL-6). LPS stimulation of RAW 264.7 macrophages occurred during the last 4 h of a 24 h incubation. The presence of the anti-inflammatory agent DEX ($10.0 \mu\text{g/ml}$) on select substrates reduced NF- κ B transcription factors responsible for the increase of IL-6. (1) -LPS; cellular growth on a glass slide. (2) -LPS; comparable growth on a Parylene A-coated slide. (3) +LPS; cellular response on a Parylene A substrate. (4) +LPS; resultant action of a DEX film upon Parylene A coating. (5) +LPS; Parylene A bilayer. (6) +LPS; Parylene A bilayer incorporated with a DEX film. (B) Gene expression of inflammatory cytokine Tumor Necrosis Factor- α (TNF- α). LPS stimulation of RAW 264.7 macrophages occurred during the last 4 h of the 24 h incubation. The presence of the anti-inflammatory agent DEX ($10.0 \mu\text{g/ml}$) on select substrates reduced NF- κ B transcription factors responsible for the increase of TNF- α . (1) -LPS; cellular growth on a glass slide. (2) -LPS; comparable growth on a Parylene A-coated slide. (3) +LPS; cellular response on a Parylene A substrate. (4) +LPS; resultant action of a DEX film upon Parylene A coating. (5) +LPS; Parylene A bilayer. (6) +LPS; Parylene A bilayer incorporated with a DEX film.

available for the deposition process. Through depriving the polymerization reaction to coat the surface in a conformal manner, pinholes form as a result.

Despite the volume of information available regarding parylene, multiple investigations pertaining to the surface characterization of micro to nanoscale deposition either have yet to be conducted or are currently ongoing. However, reports available have revealed the presence of pinholes at or below the micron level.¹³ Previous work has also indicated the elution of the underlying material from a nanoscale deposition of Parylene C.¹⁴ This information highlights the capability of parylene films to elute sequestered agents over time but also the ability to control the rate at which the material or drug is released by varying the thickness of parylene deposited. By characterizing the disposition and frequency of pinhole formation within micro to nanoscale parylene films, a greater understanding of the mechanism will lead to manipulation of the size and concentration of pores within the secondary eluting layer. The end result will be the ability to regulate drug elution over time in a site-specific concentration-dependent fashion.

In addition, recent efforts to expand upon the surface chemistry of parylene through chemical modification of the poly-*p*-xylene backbone has led to the conjugation of therapeutic

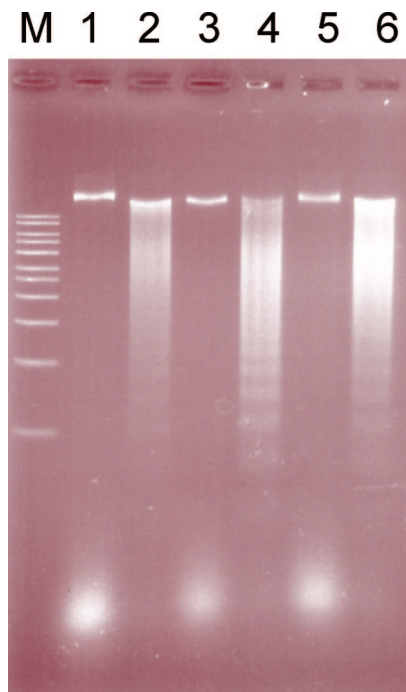


Figure 3. Electrophoretic gel depicting doxorubicin ($2.5 \mu\text{g}/\text{mL}$)-induced DNA fragmentation of RAW 264.7 macrophages. The intercalating action of doxorubicin resulted in irreparable DNA damage activating cellular apoptotic pathways. (1) Cells grown upon a plain glass slide. (2) Addition of aqueous doxorubicin to the previously indicated conditions showing fragmentation of DNA indicative of cells actively undergoing apoptosis. (3) Parylene A substrate showing no apoptotic response to the amine-functionalized surface. (4) Doxorubicin film applied to previous sample, revealing the ladder banding pattern of DNA fragmentation. (5) Parylene A bilayer revealing no significant apoptotic response to the additional secondary eluting layer. (6) Doxorubicin loaded into the Parylene A bilayer, showing apoptotic fragmentation of DNA.

agents¹⁵ and surface biotinylation.¹⁶ The presence of nonreactive functional groups on the three most prevalent types of parylene (C, N, and D) has been a limiting factor toward further modification.¹⁷ An additional benefit working with Parylene A beyond the biocompatible¹⁶ surface is the presence reactive free amine groups.

Characterization of drug elution from the Parylene A bilayer was accomplished by comparing the activity of the eluted drug to the respective controls. In all tests, elution of the drug from controls and pinhole-coated surfaces was equivalent as determined by the concentration and function of the released drug. This suggests that the secondary elution layer imposed no negative effect upon the drug function or elution. This is evident from the graphical representation of DEX-mediated gene expression in Figure 2A and B and of DOX-mediated apoptosis, demonstrated by the onset of DNA fragmentation present in Figure 3. The application of DEX has been shown to mediate downstream cytokines IL-6¹⁸ and TNF α .^{18,19} Lipopolysaccharide activation of the inflammatory cytokines IL-6 and TNF α is decreased through the presence of DEX (Figure 2A and B).

Doxorubicin functions through the intercalation of DNA²⁰ promoting cell-mediated apoptosis.^{20–22} The apoptotic behavior of RAW 264.7 cells is confirmed through the presence of laddering,²² indicative of cellular apoptosis, noted in the electrophoretic separation of DNA in Figure 3. Furthermore, Figure 3 also asserts a greater degree of biocompatibility to Parylene A. The amine-functionalized surface has no negative effect on cell growth in regards to stimulating apoptotic

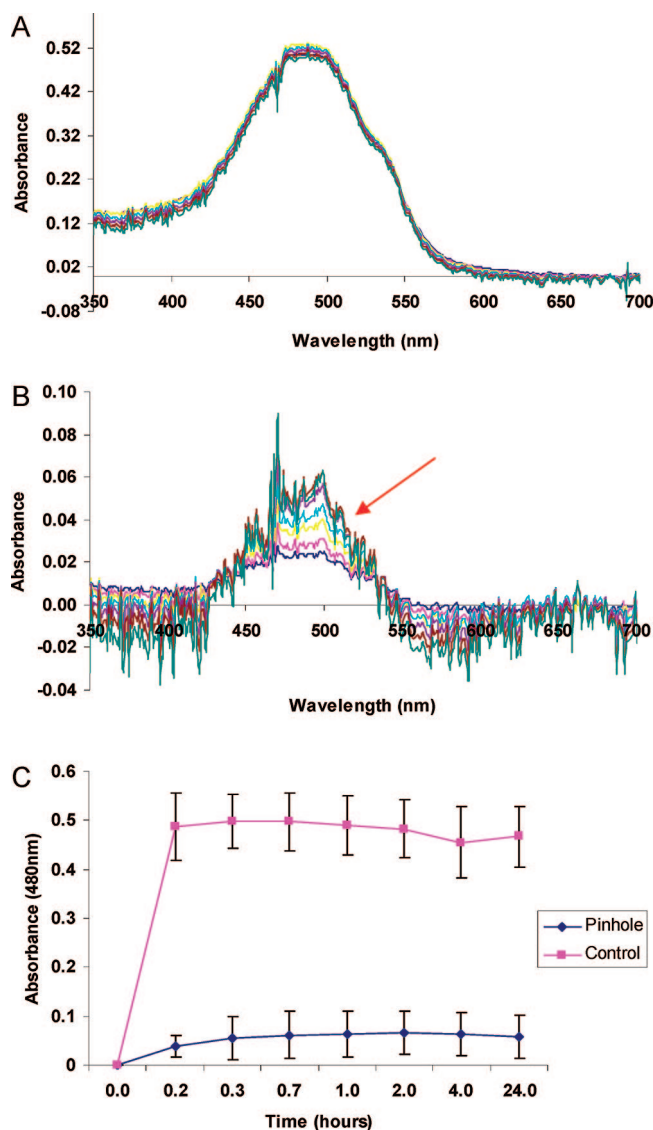


Figure 4. (A) Additive spectroscopic scans showing the complete release of DOX ($0.25 \text{ mg}/\text{mL}$) from control samples consisting of DOX applied to a base layer of Parylene A deposited on glass disks. Individual scan lines represent time points of 10, 20, and 40 min and 1, 2, 4, and 24 h. (B) Additive spectroscopic scans showing the gradual release of DOX ($0.25 \text{ mg}/\text{mL}$) from a pinhole sample consisting of DOX introduced between alternating amounts of Parylene A deposited on glass disks. Individual scan lines (inferior to superior) represent time points of 10, 20, and 40 min and 1, 2, 4, and 24 h. Restricted release of DOX reveals further evidence of the presence of pinholes when parylene is deposited at submicron or nanometer thickness. (C) Comparison of peak absorbance values (480 nm) of DOX ($0.25 \text{ mg}/\text{mL}$) elution in PBS over 24 h. Restricted release of DOX is evident as pinhole elution rates are significantly less than those of control samples. Additive measurements reflect the differential elution of the pinhole substrate and the ability of the Parylene A bilayer to restrict drug release over time.

pathways. However, clearly no positive cellular growth or activity can be garnered from the electrophoretic gel; merely the elimination of detrimental growth can be asserted.

Spectroscopic analysis revealed the degree of DOX elution over time as noted in Figure 4A–C. Compared to the control (Figure 4A), the gradual elution of DOX from alternating layers of Parylene A (Figure 4B) is evident. Further analysis integrating each sample taken at the maximum absorbance of DOX at 480 nm over time is seen in Figure 4C. Contrasting absorbance

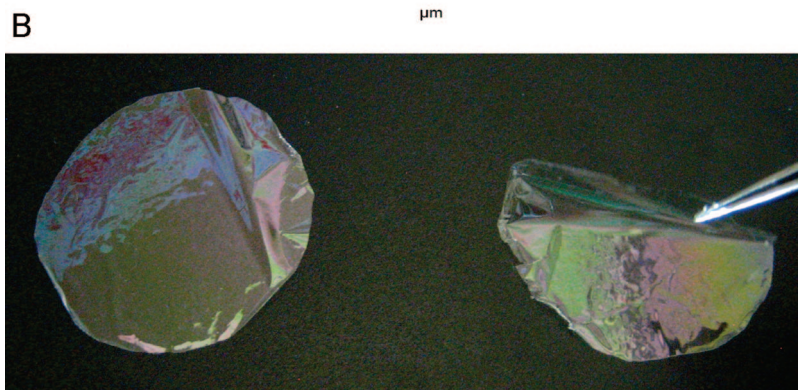
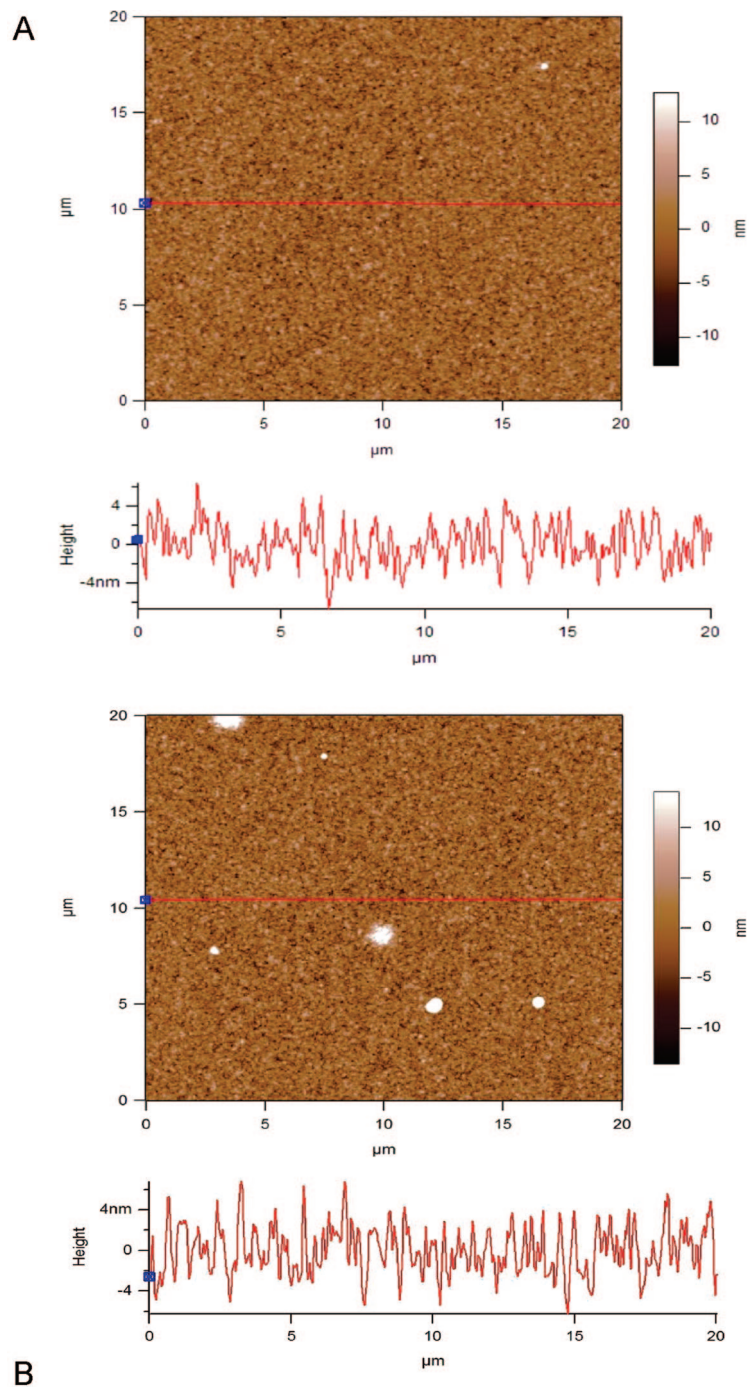


Figure 5. (A) AFM topographical image of the Parylene A base layer (top) and base layer–pinhole (bottom) substrates. Images reveal that the surface topography is unaffected by the addition of the secondary pinhole layer. The cross section graph denotes the degree of roughness present on the substrate surface. (B) Parylene A film revealing a micron thin profile. Introduction of a thin film infused with a specific therapeutic agent will allow elution of underlying drugs in a concentration-dependent site-specific manner. Advantages of such a thin film are the biocompatible nature of the material and the ultrathin profile, which suggest minimal disturbance to native tissues when implanted independently or coated onto a biomedical device.

values (Figure 4A–C) provide further evidence of the porous nature of micron to nanoscale depositions of Parylene A.

Analysis of the substrate surface utilizing AFM, present in Figure 5A, revealed that surface topography is unaffected by the addition of the pinhole elution layer. With no observed difference in the topographical analysis of the device, the data presented reveals that the microfilm form factor is preserved following the bilayer fabrication of the device. Therefore, the deposition strategy employed in this work is amenable toward the application of the device without modifications to its structure. Studies have addressed pore/pinhole imagery in poly-*p*-xylene-based surfaces, but topographical features have made it challenging to resolve pinholes.¹³ As such, this remains a source of continued research. The observation of a clear difference in the drug elution rate between the base Parylene A film and the Parylene A bilayer (Figures 2–4) demonstrates the presence of a semiporous layer. Thus, the Parylene A device is able to reduce release rates with a minimally invasive architecture that is translationally relevant.

The evidence presented affirms the presence of physical pores, present within the superficial Parylene A layer, due to incomplete polymerization of the substrate surface. Complicating the deposition of this layer to the underlying substrate is the nonadherent drug film upon the primary surface. Consequently, the secondary elution layer may shear off as a result of applied mechanical forces. This sized layer, theoretically several nanometers thick, may lack the tensile strength required to remain adherent to the substrate, resulting in delamination, thus releasing the underlying material. The potential for delamination of thin films is further exacerbated by the presence of moisture in the surrounding environment.²³ However, the data presented here, most notably the spectroscopic analysis (Figure 4A–C) support the notion of the pinhole-mediated release at the present level of parylene deposition. Delamination of the secondary layer would have resulted in bilayer elution rates comparable to that of the control.

While the precise mechanism of pinhole formation has yet to be determined, it is clear that introducing increasingly lower quantities of Parylene A into commercially available parylene deposition systems will result in the formation of porous films. It is important to note that the investigation herein has focused on porosity in regards to Parylene A. The deposition kinetics for other poly-*p*-xylene derivatives will differ significantly due to the range of functional groups and respective molecular masses.¹⁰

Noted in Figure 5B is a Parylene A film. Introducing a therapeutic patch (microfilm) or coating a biomedical device with the proposed polymer may augment existing medical treatments in a minimal, noninvasive fashion. Incorporation of an immunosuppressant such as DEX into the coating of a medical device may inhibit localized inflammation at the source of implantation, reducing scarring and expediting recovery time. Alternatively, application of an anticancer eluting device utilizing DOX may provide localized delivery of chemotherapeutic agents following postsurgical tumor excision, decreasing the incidence of tumor resurgence.

Conclusions

The application of two different classes of drugs, dexamethasone, an anti-inflammatory, and doxorubicin, a chemotherapeutic, reveals the range of medicinal agents that can be incorporated into a Parylene A polymeric device. The data presented demonstrate that the drug concentrations attained

levels comparable to their respective controls and that drug function was retained following the application of the secondary eluting layer. This platform could be configured to present a biocompatible surface with adherent biomolecules (e.g., proteins^{24,25} or other biological agents²⁶), covalently linked to surface amine groups, while maintaining site-specific drug-eluting properties. Clearly, further investigations are warranted to characterize the porous nature of micron to nanoscale depositions of parylene. This investigation creates a foundation from which the field can expand onto future prospects in regards to the next generation of differentially modified poly-*p*-xylene alternatives.

Acknowledgment. The authors gratefully acknowledge support from a V Foundation for Cancer Research V Scholar Award, a National Science Foundation Center for Scalable and Integrated NanoManufacturing (SINAM) Grant DMI-0327077, and a National Institutes of Health Grant U54 A1065359. Additionally, the authors would like to thank Robert Lajos of the Nanotechnology Core Facility at the University of Illinois at Chicago as well as James Brundage of Uniglobe Kisco.

References and Notes

- (1) Eskin, S. G.; et al. *J. Biomed. Mater. Res.* **1976**, *10*, 113.
- (2) Fontaine, A. B.; Koelling, K.; Dos Passos, S.; Cearlock, J.; Hoffman, R.; Spigos, D. G. *J. Endovas. Surg.* **1996**, *3*, 276.
- (3) Chang, T. Y.; Yadav, V. G.; DeLeo, S.; Mohedas, A.; Rajalingam, B.; Chen, C. L.; Selvarasah, S.; Dokmeci, M. R.; Khademhosseini, A. *Langmuir* **2007**, *23*, 11718.
- (4) Fortin, J. B.; Lu, T. M. *Chemical Vapor Deposition Polymerization: The Growth and Properties of Parylene Thin Films*; Kluwer: Norwell, MA, 2004.
- (5) Dolbier, W. R.; Beach, W. F. *J. Fluorine Chem.* **2003**, *122*, 97.
- (6) Bruck, S. D. *Blood Compatible Synthetic Polymers*; CC Thomas: Springfield, IL, 1974.
- (7) Westedt, U.; Wittmar, M.; Hellwig, M.; Hanefeld, P.; Greiner, A.; Schaper, A. K.; Kissel, T. *J. Controlled Release* **2006**, *111*, 235.
- (8) Unger, F.; Westedt, U.; Hanefeld, P.; Wombacher, R.; Zimmermann, S.; Greiner, A.; Ausborn, M.; Kissel, T. *J. Controlled Release* **2007**, *117*, 312.
- (9) Hildebrand, H. F.; Blanchemain, N.; Mayer, G.; Chai, F.; Lefebvre, M.; Bosch, F. *Surf. Coat. Technol.* **2006**, *200*, 6318.
- (10) Kramer, P.; et al. *J. Polym. Sci.* **1984**, *22*, 475.
- (11) Yang, G. R.; Ganguli, S.; Karcz, J.; Gill, W. N.; Lu, T. M. *J. Cryst. Growth* **1998**, *183*, 385.
- (12) Brody, J. R.; Kern, S. E. *Biotechniques* **2004**, *36*, 214.
- (13) Spellman, G. P.; Carley, J. F.; Lopez, L. A. *J. Plast. Film Sheeting* **1999**, *15*, 308.
- (14) Zeng, J.; Aigner, A.; Czubayko, F.; Kissel, T.; Wendorff, J. H.; Greiner, A. *Biomacromolecules* **2005**, *6*, 1484.
- (15) Lahann, J.; Klee, D.; Plueter, W.; Hoecker, H. *Biomaterials* **2001**, *22*, 817.
- (16) Miwa, J.; Suzuki, Y.; Kasagi, N. *Evaluation of Cell Velocity Regulation in a Microfabricated Adhesion-Based Cell Separation Device*; Proceedings of the International Conference on Microtechnologies in Medicine and Biology, Okinawa, Japan, 2006.
- (17) Yoshida, M.; Langer, R.; Lendlein, A.; Lahann, J. *Polym. Rev.* **2006**, *46*, 347.
- (18) Jeong, H.-J.; Na, H.-J.; Hong, S.-H.; Kim, H.-M. *Endocrinology* **2003**, *144*, 4080.
- (19) Maeda, K.; Yoshida, K.; Ichimiya, I.; Suzuki, M. *Hear. Res.* **2005**, *202*, 154.
- (20) Jurisicova, A.; Lee, H. J.; D'Estaing, S. G.; Tilly, J.; Perez, G. I. *Cell Death Differ.* **2006**, *13*, 1466.
- (21) Wang, S.; Kotamraju, S.; Konorev, E.; Kalivendi, S.; Joseph, J.; Kalyanaraman, B. *Biochem. J.* **2002**, *367*, 729.
- (22) Huang, H.; Pierstorff, E.; Osawa, E.; Ho, D. *Nano Lett.* **2007**, *7*, 3305.
- (23) Waters, P.; Volinsky, A. *Exp. Mech.* **2007**, *47*, 163.
- (24) De Bartolo, L.; Morelli, S.; Piscioneri, A.; Lopez, L. C.; Favia, P.; d'Agostino, R.; Drioli, E. *Biomol. Eng.* **2007**, *24*, 23.
- (25) Lopez, L. C.; Gristina, R.; Ceccone, G.; Rossi, F.; Favia, P.; d'Agostino, R. *Surf. Coat. Technol.* **2005**, *200*, 1000.
- (26) Hoffman, A. S. *Clin. Chem.* **2000**, *46*, 1478.